Quench Absorption Coils: A Quench Protection Concept for High-field Superconducting Accelerator Magnets

M. Mentink[1], T. Salmi[2]

[1]CERN, CH-1211 Geneva 23, Switzerland

[2]Tampere University of Technology, 33720 Tampere, Finland

E-mail: mmentink@cern.ch

Abstract.

A quench protection concept based on coupled secondary coils is studied for inductively transferring energy out of quenching superconducting dipole and thus limiting the peak hotspot temperature. So-called 'quench absorption coils' are placed in close proximity to the superconducting coils and are connected in series with a diode for the purpose of preventing current transformation during regular operation. During a quench, current is then transformed into the quench absorption coils so that a significant fraction of the stored magnetic energy is dissipated in the these coils.

Numerical calculations are performed to determine the impact of such a concept and to evaluate the dimensions of the quench absorption coils needed to obtain significant benefits. A previously constructed 15 T Nb_3Sn block coil is taken as a reference layout. Finite-element calculations are used to determine the combined inductive and thermal response of this system and these calculations are validated with a numerical model using an adiabatic approximation.

The calculation results indicate that during a quench the presence of the quench absorption coils reduces the energy dissipated in the superconducting coils by 45 % and reduces the hotspot temperature by over 100 K. In addition, the peak resistive voltage over the superconducting coils is significantly reduced. This suggests that this concept may prove useful for magnet designs in which the hotspot temperature is a design driver.

1. Introduction

As part of future upgrades for CERN accelerator physics, such as the high energy large hadron collider (HE-LHC) [1, 2] and the future circular collider for hadron-hadron physics (FCC-hh) [3], superconducting dipoles that produce ever higher magnetic fields are required. An effort is under way to determine whether reliable and affordable production of Nb_3Sn-based 16 T dipoles is attainable. In addition to other challenges, such as very high mechanical stresses, the need for cost reduction, and field quality considerations, protecting the integrity of these dipoles in case of a quench is an important design consideration. Because of the high cost of the superconducting cable,

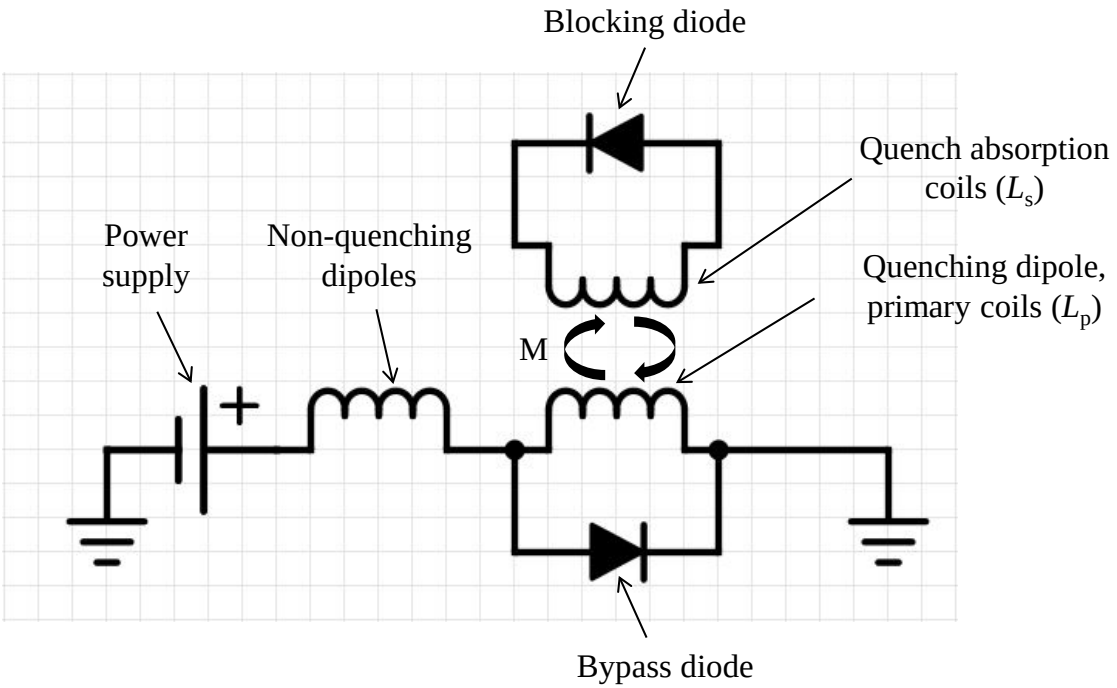

Figure 1. Simplified electrical circuit representing the quench dipole with superconducting and quench absorption coils, the other dipoles in the circuit, the bypass diode which conducts part of the current during a quench, and the blocking diode which prevents transformation of current to the quench absorption coils during ramping. The quench absorption coils comprise insulated copper windings where all windings are assumed be part of a single current loop and are placed in series with a diode. The energy extractors used for discharging the non-quenching dipoles are omitted from this circuit.

it is desirable to limit the size of the superconducting coils. A conflicting consideration is the need to homogeneously distribute the stored energy over a sufficiently large volume during a quench, thus limiting the hotspot temperature.

In this paper, a concept is explored which seeks to meet these two apparently conflicting goals. The concept relies on placing copper-based coils in close proximity to the superconducting coils, so that in case of a quench a significant amount of the stored energy in the superconducting coils is dissipated in these so-called quench absorption coils. Variants of this concept have been described and applied in the past [4, 5, 6, 7, 8]. Here, the quench absorption coils are placed in series with a blocking diode that prevent current transformation below a critical current ramp-rate threshold dI_c/dt given by the diode voltage threshold, thus preventing heating and induced field errors during a regular ramp. At the same time the threshold voltage over the diode is small with respect to the inductive voltage over the quench absorption coils during a quench, so that in that case the influence of the diode on the inductive response of the system is minimal. This diode is to be integrated with the cold mass, as was done with the dipoles of the Large Hadron Collider [9].

To investigate such a concept for use in high-field superconducting dipoles, the LBL HD2 block coil geometry [10, 11] is taken, and the quench behavior with and without quench absorption coils is analyzed. This 15 T superconducting dipole is a Nb_3Sn-based prototype with which the designers sought to push the limit of accelerator magnet technology towards the high magnetic field regime suitable for future particle colliders such as HE-LHC [1, 2] and FCC-hh [3].

This paper is subdivided into sections in which the following topics are discussed: The electrical circuit (section 2), the HD2 geometry and magnetic field (section 3), the calculation method (section 4), the calculation results (section 5), the influence of the coupling factor (section 6), some design variations (section 7), additional benefits of quench absorption coils beyond limiting hotspot (section 8), a general discussion (section 9) and finally the conclusions (section 10).

2. Electrical circuit

Fig. 1 shows a schematic of the electrical circuit of the system, indicating the superconducting and quench absorption coils, the diodes and the additional non-quenching dipole magnets in the system. Analogous to the superconducting windings, all windings in the quench absorption coils are assumed to be in series with each other and with a single cold (i.e. operating at 1.9 K) diode.

In particle accelerators, it is common to connect the superconducting dipoles in series, thus reducing the required amount of power supplies and current leads. The dipole magnets are placed parallel to bypass diodes, which temporarily allows current to bypass a quenching dipole while the remaining non-quenching dipoles in the circuit are discharged over energy extractors [9]. The addition of quench absorption coils is compatible with this concept and requires the addition of a so-called blocking diode for each dipole (Fig. 1).

The voltage threshold of the blocking diode is made sufficiently high to block current transformation during ramping of non-quenching dipoles. This value is thus determined by the desired peak discharge rate of the non-quenching dipoles and is discussed in section 9.

For the purpose of the quench simulations, the threshold voltage of the by-pass diode is considered negligible, so that superconducting coils may be considered shorted. This implies that the quench behavior of the quenching dipole may be considered as independent of the other dipoles in the system. In addition, the threshold voltage of the blocking diode is considered negligible during a quench, which is justified in section 9.

3. HD2-like high-field Nb_3Sn block coil with quench absorption coils

To investigate the potential advantage of using quench absorption coils in high-field Nb_3Sn dipoles, the example of a previously constructed high-field magnet HD2 is taken [11]. Fig. 2 shows a two-dimensional approximate reproduction of the magnetic field

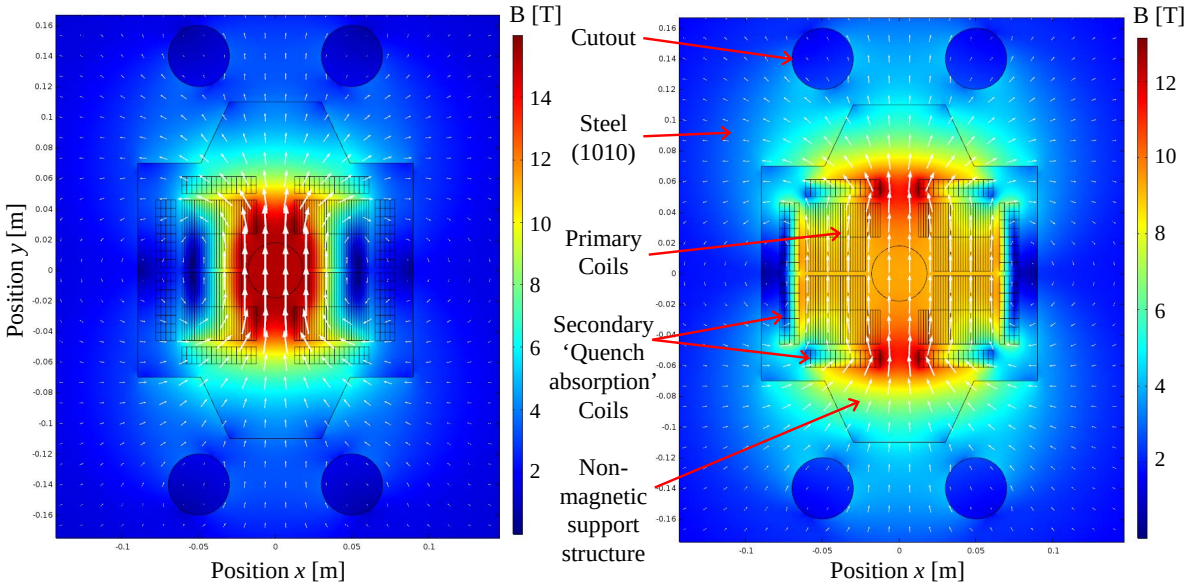

Figure 2. Magnetic fields generated by HD2 in combination with the quench absorption coils. In the left figure, the superconducting coils of HD2 are energized with an operating current of 17.3 kA and the quench absorption coils do not carry any current. In the right figure, the superconducting coils carry no current and the quench absorption coils carry 14 kA. In both cases, the stored magnetic energy of the system is 840 kJ/m.

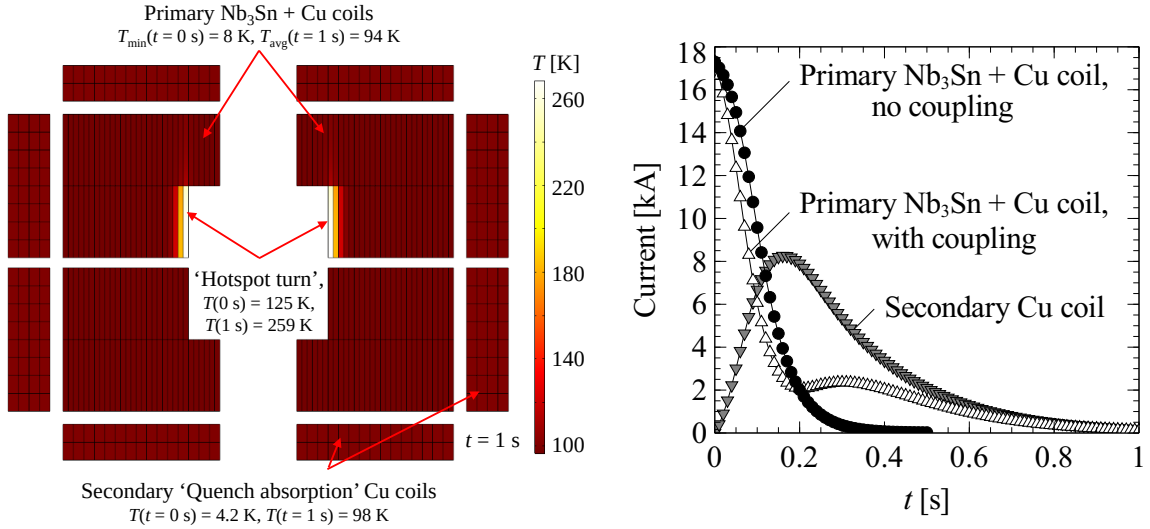

Figure 3. Thermal + inductive simulation results of the superconducting dipole with quench absorption coils. Left: Temperature distribution after 1 s. Right: Time-dependent current during a quench in the primary and secondary circuit, also showing the resulting current in the primary circuit when quench absorption coils are absent.

produced by HD2 using Comsol Multiphysics [12]. Here some of the fine features in the original design (in particular the various cutouts in the iron yoke surrounding the superconducting coils) are omitted. Fig. 3 shows only the windings of the

superconducting coils and the quench absorption coils. Analogous to the three-dimensional geometry of the superconducting coils themselves (see for instance [11]), the quench absorption coils are assumed to be race-track coils with flared ends to allow for passage of the beam-tube at the ends of the cold mass.

The operating current of the dipole is 17.3 kA and the dimensions of the Rutherford cable (including insulation) are 22.2 × 1.6 mm. The Rutherford is assumed to comprise 36 vol.% Nb_3Sn, 35 vol.% copper, and 15 vol.% G10, where the remaining 13 vol.% is void-space. Also shown are the quench absorption coils, which occupy some of the space that was occupied by bronze and stainless steel support structure in the original HD2 design. The quench absorption coils comprise insulated copper windings with dimensions of 5.6 mm × 3.2 mm. The insulation thickness between adjacent windings is taken at 220 μm, so that these copper windings comprise 88 vol.% copper and 12 vol.% G10. The magnetic properties of the iron yoke is taken as the ST1010 steel used for ATLAS [13]. Hysteresis in the magnetic behavior of the iron is not considered.

Fig. 2, left, shows the magnetic field generated when the superconducting coils are powered at 17.3 kA and no current is present in the quench absorption coils. In this case, the average field in the bore is 15.2 T, the peak field on the conductor is 16.0 T, the average field on the coil windings is 7.9 T, the average field in the quench absorption coil windings is 5.9 T, and the stored energy is 0.84 MJ/m. The stored energy matches the stored energy in the original design, while the average field in the bore and the peak field on the conductor are about 0.2 T higher than in the original design. This difference in magnetic field magnitude may be explained in terms of minor geometrical differences as well as the non-linear magnetic properties of the iron yoke.

When all the magnetic stored energy is transferred to the quench absorption coils (which, similar to the superconducting coils are all assumed to be in series), 14 kA is needed to obtain the same magnetic stored energy. In this case the average field in the windings of coils is 8.8 T and the 6.3 T for the superconducting coils and quench absorption coils, respectively. The residual resistivity ratio of the copper in the superconducting coils is assumed equal to 100, whereas the copper in quench absorption coils is assumed to be half-hard copper with a residual resistivity ratio of 80. Considering the magneto-resistivity of copper, the average residual resistivity ratios of both coils in magnetic field is then about 40. For the purpose of calculating dissipation, it is assumed that the copper solely determines the resistance, which is reasonable as the normal state resistivity of copper in magnetic field is over 300 and 50 times lower than Nb_3Sn at 20 K and 300 K, respectively.

From the magnetic calculation results, the self- and mutual inductances per meter of the superconducting and quench absorption coils are determined. Due to saturation in the iron, the self- and mutual inductances are current dependent. Moreover, the combined self-inductance of the superconducting coils is not only dependent on the current in the primary circuit, but also that of the secondary and vice versa. However, the non-linear impact of the iron is somewhat modest as removal of the iron reduces the stored energy by less than 20 %. For the sake of limiting the complexity of the

simulations the non-linearity resulting from the iron is ignored so that all inductances are taken as constants. The non-linear effect of the iron yoke on the inductances thus constitutes an uncertainty in the modelling approach taken here.

The constant inductances are found by evaluating the current needed for all the stored energy to be located in either the superconducting coils (Fig. 2, left) or the quench absorption coils (Fig. 2, right). The self-inductances are then calculated with:

$$U_{\text{stored}} = 0.5LI^2, \tag{1}$$

where U_{stored} is the stored magnetic energy per meter, L is the self-inductance, and I is the current. This gives self-inductances of 5.6 mH/m and 8.6 mH/m for the superconducting and quench absorption coils, respectively. The mutual inductance is found by calculating the coupling factor in the absence of the iron yoke yielding 76 %, thus indicating an effective mutual inductance of 5.3 mH/m. Calculating the effective coupling factor in this manner is somewhat pessimistic, as the presence of the iron yoke may be expected to lead to enhanced coupling between the superconducting and quench absorption coils. The influence of the effective coupling factor is addressed in section 6.

4. Thermal + inductive simulation method

Two different types of calculations are performed to see how quench behavior is affected by the presence of quench absorption coils. Both models assume an infinitely long dipole which is approximated with a two-dimensional geometry.

The first simulation uses finite element analysis, where thermal exchange between adjacent layers is considered. Time-dependent finite-element calculations are done in Comsol Multiphysics [12], combining the 'Heat Transfer' module and the 'Global ODEs and DAEs' module. In the latter, the inductive coupling between the primary and secondary circuits is described with the following equations:

$$L_{\text{p}}dI_{\text{p}}/dt(t) + MdI_{\text{s}}/dt(t) + P_{\text{p}}(t)/I_{\text{p}}(t) = 0, \tag{2}$$

$$L_{\text{s}}dI_{\text{s}}/dt(t) + MdI_{\text{p}}/dt(t) + P_{\text{s}}(t)/I_{\text{s}}(t) = 0, \tag{3}$$

where L_{p} and L_{s} are the self-inductances per meter of the two circuits, M is the mutual inductance per meter, P_{p} and P_{s} are the time-dependent rates of dissipation per meter, and I_{p} and I_{p} are the time-dependent currents.

In the 'Heat transfer' module, the composition of the superconducting and quench absorption coils are considered to yield the temperature dependent volumetric heat capacity, resistivity, and thermal conductivity. The relevant physical properties are taken from literature [14, 15, 16, 17, 18].

In principle, to determine the hotspot temperature one should consider the time needed before a quench is detected and validated and the time required for the protection system to homogeneously quench the superconducting coils (using either quench heaters, CLIQ [19], or some other method). However, as the main purpose of this paper is to

illustrate the concept of quench absorption coils and investigate the feasibility of this concept in a simplified manner, such an analysis is considered beyond the scope of this paper. Instead it is assumed that at $t = 0$ s the quench has been detected and heat has been homogeneously distributed into the superconducting coils (yielding a temperature of 8 K throughout the coils at which the coils are assumed to be entirely normal) and a 'hotspot turn' is assumed to already be at an elevated temperature. Thus, this analysis gives no indication of the efficiency of the method used for inducing a homogeneous quench throughout the superconducting coils, but the impact of this efficiency may be investigated by adjusting the temperature of the hotspot turn at $t = 0$ s.

In the second numerical analysis, the local heating in the conductor is assumed to be adiabatic (i.e. the thermal resistance of the G10 surrounding conductor is assumed to be infinite), so that the thermal and inductive behavior may be described with relatively straightforward numerical equations. This second model serves as a consistency check, as the calculation results should be nearly identical when the thermal resistance between adjacent windings is made very high in the first model. In this case the inductive and thermal behavior may be described with equations 2 and 3 in addition to the following set of equations:

$$P_{\mathrm{p}}(t) = (I_{\mathrm{p}}(t)/A_{\mathrm{cond,p}})^2 \rho_{\mathrm{p}}(T) A_{\mathrm{p}}, \tag{4}$$

$$P_{\mathrm{s}}(t) = (I_{\mathrm{s}}(t)/A_{\mathrm{cond,s}})^2 \rho_{\mathrm{s}}(T) A_{\mathrm{s}}, \tag{5}$$

$$dT_{\mathrm{p}}/dt(t) = P_{\mathrm{p}}(t)/(C_{\mathrm{V,p}}(T) A_{\mathrm{p}}), \tag{6}$$

$$dT_{\mathrm{s}}/dt(t) = P_{\mathrm{s}}(t)/(C_{\mathrm{V,s}}(T) A_{\mathrm{s}}), \tag{7}$$

where $\rho_{\mathrm{p}}(T)$ and $\rho_{\mathrm{s}}(T)$ are the temperature-dependent resistivities, A_{p} and A_{s} are the cross-sectional areas of the superconducting and quench absorption coils, and $C_{\mathrm{V,p}}(T)$ and $C_{\mathrm{V,s}}(T)$ are the temperature-dependent volumetric heat capacities of the superconducting and quench absorption coils. The second model is essentially a variation of the so-called MIITS concept [20], with an added consideration for inductive coupling. Under the assumption of a homogeneous quench where the volume of the hotspot is considered small, the time-dependent current is calculated. The peak hotspot temperature is then determined by assuming an elevated hotspot temperature at $t = 0$ s and calculating the local temperature rise, taking the time-dependent current as input.

5. Calculation results

5.1. Comsol results

Fig. 3, left shows the geometry used in the thermal simulation, comprising both the superconducting coils and the quench absorption coils. At the start of the simulation the temperatures of the superconducting coils, the quench absorption coils, and hotspot turn is fixed to 8, 4.2, and 125 K, respectively. After 1 s, the temperatures are 94, 98, and 259 K, respectively. Fig. 3, right shows the time-dependent current in the

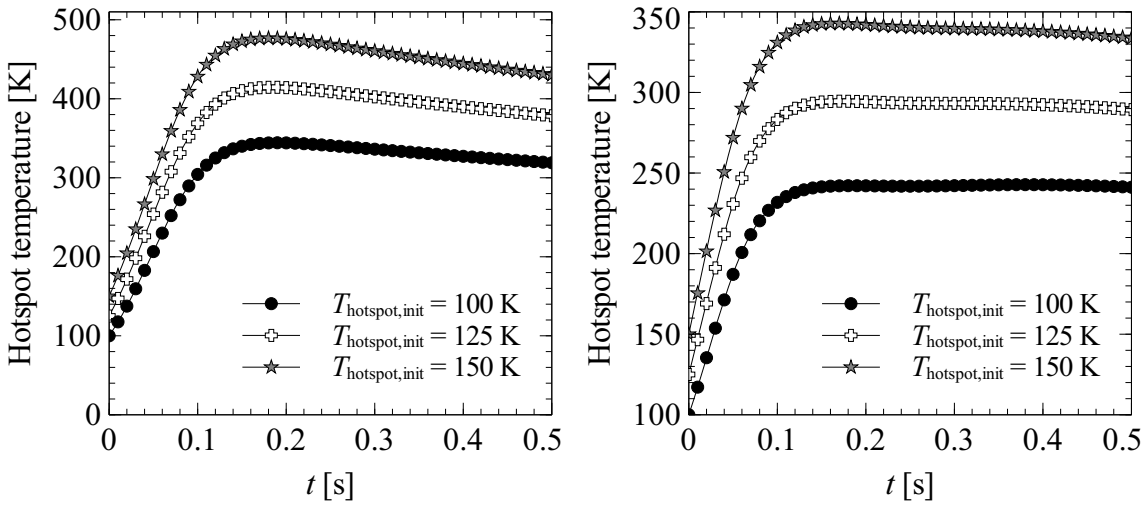

Figure 4. Hotspot temperature as a function of time under varying starting conditions. The left figure shows calculation results where the quench absorption coils are omitted and the right figure shows results where the quench absorption coils are included.

superconducting and quench absorption coils, compared to the situation in which the quench absorption coils are absent. In Fig. 4, a comparison of hotspot temperatures is made in the cases where the quench absorption coils are either absent (Fig. 4, left) or present (Fig. 4, right) at three different starting hotspot temperatures.

Clearly the peak hotspot temperature is significantly reduced in the presence of quench absorption coils. To illustrate, at a starting hotspot temperature of 125 K, the peak hotspot temperature is 414 K when quench absorption coils are not present (Fig. 4, left) and 295 K when they are (Fig. 4, right), which is a hotspot temperature reduction exceeding 100 K. This reduction can be explained through the difference in time-dependent current (Fig. 3, right). Without the quench absorption coils the current in the primary circuit drops to 50 % of the operating current after 108 ms, whereas this number drops to 77 ms when the influence of the quench absorption coils is considered.

It may seem surprising to see that the final temperature in the quench absorption coils of 98 K is in fact higher than that in the superconducting coils (Fig. 3, left), in spite of the nearly 40 % higher heat capacity per unit volume in the quench absorption coils. This result follows from the nearly three times lower normal state resistivity in the quench absorption coils due to the much higher copper fraction, which allows the quench absorption coils to temporarily 'hold' a relatively large amount of current. This somewhat counter-intuitive result is more apparent when it is considered that the maximum current in the quench absorption coils is the current at which the inductive voltage (MdI_{p}/dt) over the secondary circuit is equal to the resistive voltage. A lower resistivity then leads to a larger maximum current and the dissipated power is the product of the current and the resistive voltage, so that a lower resistivity implies higher power dissipation. The result is that even though the quench absorption coils

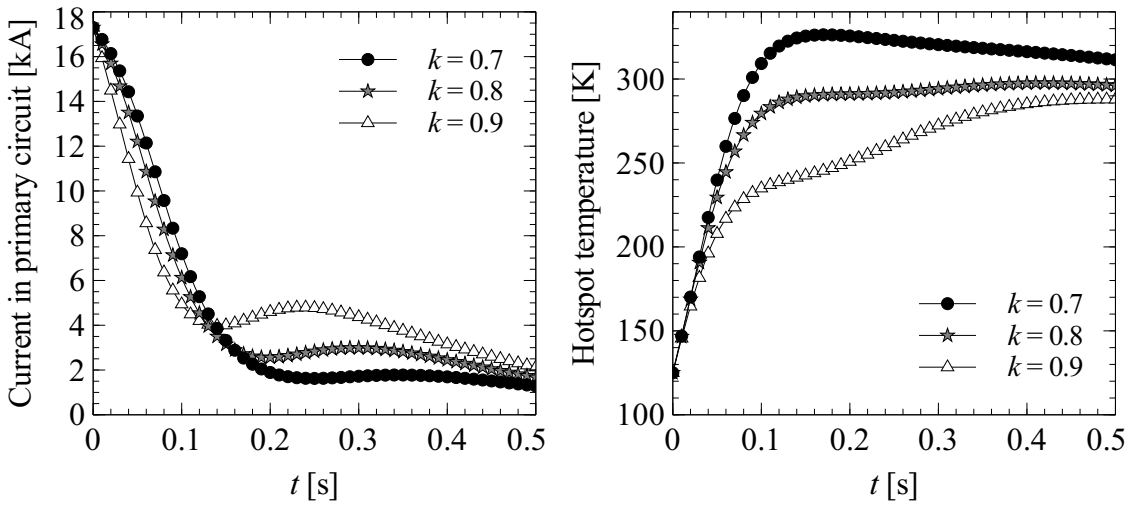

Figure 5. The impact of the coupling factor k on the quench discharge behavior. The left figure shows the time-dependent current and the right figure shows the time-dependent hotspot temperature.

only constitute 36 % of total winding volume, 45 % of the stored energy is dissipated in these coils.

The difference in peak hotspot temperatures between the two cases with and without quench absorption coils increases with increasing hotspot temperature, with 344, 414, and 476 K in the absence of quench absorption coils, and 242, 294, and 342 K in the presence of quench absorption coils, for starting hotspot temperatures of 100, 125, and 150 K, respectively.

5.2. Adiabatic numerical consistency check

In the adiabatic limit, i.e. where the thermal resistance between adjacent conductors is made very large, the results of the two models described in section 4 may be compared. The results are found to be consistent within four Kelvin, with a final hotspot temperature of 335 K, a superconducting coil temperature of 95 K, and a final quench absorption coil temperature of 99 K, if a starting hotspot temperature of 125 K is assumed. In the absence of the quench absorption coils, the results are also consistent at 428, 125, and 4.2 K, respectively.

6. Influence of the coupling factor

A topic which is not thoroughly addressed in this paper is how the presence of the iron yoke affects the coupling factor.

Similar to the role of a weak-iron core in a transformer, one may expect the effective coupling factor k to increase in the presence of iron. This is beneficial for the efficiency of the quench absorption coils as the inductive response time is reduced and the inductive voltage over the secondary circuit is enhanced. With higher values of k, the current

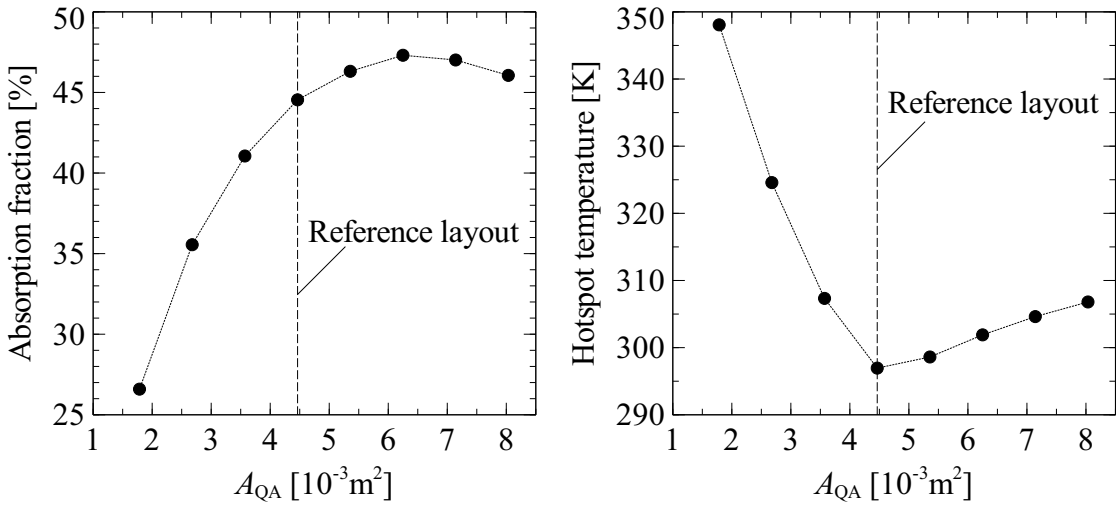

Figure 6. Left: Fraction of the total stored magnetic energy absorbed by the quench absorption coils as a function of coil cross-section. Right: Peak hotspot temperature as a function of quench absorption coil cross-section.

decay rate in the primary circuit increases (Fig. 5, left), which results in a decreased peak hotspot temperature (Fig. 5, right). The difference in peak hotspot temperature is somewhat modest; increasing the coupling factor from 70 % to 90 % results in a 40 K reduction in peak hotspot temperature. Thus the assumed constant coupling factor k used in the calculations is somewhat simplistic, but applying the physically more accurate current-dependent k would not significantly alter the implications of using quench absorption coils.

An interesting phenomenon is observed in Fig. 5 in which current is transformed back into the primary circuit after current saturation of the secondary circuit, particularly for higher values of k. This phenomenon may be understood as a thermal lag in the quench absorption coils, resulting in a relatively low initial normal state resistivity and thus a greater current carrying capacity. Then, as the quench absorption coils catch up to the superconducting coils in terms of temperature and resistance, some current is transferred back into the primary circuit.

7. Design variations

A parameter study is performed to investigate the relationship between the size of the quench absorption coils and their efficiency in reducing the hotspot temperature, where the amount of windings is fixed but their dimensions are modified.

In the relationship between the size of the quench absorption coils and the resulting absorption fraction and hotspot temperature, two competing effects are relevant. First of all, the size and heat capacity of the quench absorption coils limit the amount of energy that can be dissipated there during a quench as the current in the secondary circuit stops rising once the inductive voltage (MdI_p/dt) is equal to the resistive voltage. In this

sense larger quench absorption coils are preferable. At the same time, the time needed to transfer the current is determined by the effective inductance of the superconducting coils, i.e. $L_{\mathrm{p}}(1-k^2)$, and the resistive voltage over the primary circuit. Larger quench absorption coils lead to a smaller coupling factor, as the produced magnetic field has lesser overlap with that of the superconducting coils. To illustrate, increasing the size of the quench absorption coils by 80 % with respect to the reference design (Fig. 3, left) results in a reduction of the coupling constant from 76.4 % down to 73.2 %.

The results of this parameter study are shown in figure 6. In terms of the absorption fraction, the optimal amount is found when the quench absorption coils are increased by 40 % with respect to the reference design. In terms of hotspot temperature however, the reference design seems to be optimal. The occurrence of two different optimal values for absorption fraction and hotspot temperature is related to the fact that for the peak hotspot temperature the thermal exchange between neighboring cables also plays a role, i.e. a time-dependent effect, so that both absorption fraction and inductive time constant determine the peak hotspot temperature. Given that the goal of optimization was to reduce the peak hotspot temperature, the size of the quench absorption coils in the reference design seems appropriate.

8. Additional benefits of quench absorption coils

In addition to limiting the energy dissipated in the superconducting coils themselves, and thus limiting the hotspot temperature, the quench-absorption-coil concept also gives additional benefits.

First, the presence of the quench absorption coils reduces the effective inductance of the superconducting coils, so that the turn-to-turn voltage is reduced during a quench. The turn-to-turn voltage is related to the manner in which the layers are connected, but as a useful proxy one may consider the total resistive voltage per meter. In the absence of quench absorption coils this voltage peaks at 707 V/m, whereas their presence reduces this to 347 V/m. Another way to understand is that due to the presence of quench absorption coils a smaller fraction of the stored energy is dissipated in the superconducting coils and the resistive voltage is reduced as well. Thus, the minimum required electrical performance of the electrical insulation is more forgiving when quench absorption coils are present.

Another less obvious benefit is that the magnetic coupling between the primary and secondary circuit may be used for monitoring purposes. Similar to so-called “pick-up coils” (See for instance [21, 22, 23]), one may balance the inductive voltage drop over the top quench absorption coils versus that of the bottom coils, so that the occurrence of magnetic perturbations in the superconducting coils may be observed. This may allow for additional means to improve the reliability of quench detection.

9. Discussion

An implicit assumption in the models is that the thermal behavior of the magnet may be represented with two-dimensional geometry. Justification for the two-dimensional approximation of the magnet geometry is given by the fact that the aspect ratio of accelerator dipoles are quite large. For instance, the superconducting windings of a single aperture of the LHC NbTi dipole are contained within a 60 mm radius, while the cold mass length is 14 meters [24]. The thermal conductivity is also distinctly anisotropic: The axial thermal conductivity is dominated by copper while the transverse thermal conductivity is dominated by the G10 insulation, and the ratio of the thermal conductivities of these two material is about 5000 at 4.2 K. Finally, a homogeneous quench is assumed to be initiated by quench heaters which are distributed along the length of the magnet, so that in general the temperature may be assumed to be homogeneous along the length of the windings. Note that the 'hot-spot turn' approximation is somewhat simplistic, as a hot-spot is initially a local phenomenon. However, this does not affect the current transformation between coils as the resistive voltage drop over a single turn is small compared to the total resistive voltage drop over the superconducting coils once they are in normal state. From a peak hotspot temperature perspective a 'hotspot turn' is more pessimistic than an assumed local hotspot in a fully three-dimensional model, as in the latter case heat from the hotspot may diffuse along the length of the winding. At the same time it is less pessimistic than the adiabatic approximation (see section 5.2) in which heat diffusion is suppressed altogether.

While the concept of quench absorption coils is beneficial from a quench protection perspective, this concept does come at a price. The quench absorption coils occupy space which would otherwise be used for support structure, and winding these coils would introduce another manufacturing step in an already complicated manufacturing process. In addition, the presence of the quench absorption coil does not enhance the stability of the conductor, which means that one cannot immediately assume that this concept may be used to significantly reduced the copper fraction of the superconducting cable, thus shrinking the superconducting coils. However, the impact on the peak hotspot temperature is significant, which means that in the scenario where peak hotspot temperature is a design driver (which is true for dipole designs for FCC-hh [25]), it may lead to a overall cost reduction for these dipoles. To illustrate, to limit the hotspot temperature to below 350 K, the preliminary designs of the FCC-hh Common-Coil dipole [26], the cosinus-theta design [27], and the block coil design [28] all use at least one Nb_3Sn conductor with a copper-to-noncopper ratio ranging between 1.6 and 3.5.

The mechanical implications of adding these quench absorption coils are currently not clear. If one assumes that they are wound on to the structure after the heat treatment is completed (so that the heat treatment does not affect the mechanical properties of the copper), then a combination of good electrical and mechanical properties is possible. This implies that the quench absorption coils may be used for

transferring force and constraining the superconducting coils. To illustrate, the residual resistivity ratio of 60 % cold-worked copper is as high as 75, while the measured yield strength is 475 MPa and the ultimate tensile strength is 514 MPa at 4 K [17]. In addition, no voids or brittle material is present inside the quench absorption coils, so that reasonable mechanical properties may be expected. It is clear that proper mechanical support of the superconducting coils is paramount, so that further research on the mechanical implications of applying this concept is required.

Even though the quench absorption coils are connected in series with a diode the diode threshold voltage is neglected in the quench discharge calculations. This approach seems reasonable. If, similar to the LHC all non-quenching dipoles are discharged with a time constant on the order of 100 s [9] during a fast power abort, this implies that blocking diode should allow for a ramp-rate of 173 As^{-1}, thus implying a diode threshold of 0.74 V per meter of dipole. In comparison, the dissipation during a quench is on the order of several hundred volts per meter of the dipole. Thus, the influence of the diode on the electrical response during a quench is quite small.

It should be noted that while the diodes prevent current transformation during regular operation, it does not prevent internal eddy currents inside the conductor in the quench absorption coils. However, this effect is small: Using an analytical estimate of eddy currents [29] with a regular ramp rate of 9.6 A/s, total eddy current heating of 0.48 μW/m is found in the quench absorption coils per meter of dipole.

The quench absorption coil concept is complementary to extraction with a dump resistor, as the additional voltage drop over the primary circuit enhances current transformation onto the secondary circuit. This aspect is not emphasized in this paper, as implementing a meaningful amount of extraction in a string of dipoles in a future accelerator complex is likely difficult due to the large combined stored energy. An interesting proposal was recently published in which cold energy extraction is applied in a distributed manner, so that meaningful extraction can be achieved without the associated large voltages [30]. Each dipole can then have a dump resistor which is decoupled from the other non-quenching dipoles. To illustrate the complimentary nature of energy extraction and quench absorption coils, one may compare a dipole that is quenching without a dump resistor to a dipole which is discharged over a dump resistor with a peak extraction voltage of 200 V/m. Without quench absorption coils, 28.4 % of the stored energy is dissipated in the dump resistor during a quench. Regardless of whether a the dump resistor is included in the circuit, about 45 % of the stored energy is dissipated in the quench absorption coils, which may be understood in terms of a reduced resistive voltage drop over the superconducting coils and an additional voltage drop over the dump resistor. The addition of the dump resistor reduces the fraction of total stored energy dissipated in the superconducting coils from 55 % to 35 % of the stored energy, i.e. a 36 % reduction. For a starting hotspot temperature of 125 K, this leads to a further 44 K reduction in the peak hotspot temperature to 251 K.

It is interesting to consider how quench absorption coils relate to CLIQ [19] as both concepts rely on inductive coupling. CLIQ relies on applying an oscillating magnet field

to the conductor, resulting in inter-filamentary coupling currents and volumetric heating. One may speculate that the presence of quench absorption coils does not necessarily affect the operation of CLIQ. For instance, if the top superconducting coils are made to oscillate against the bottom superconducting coils, then due to symmetry the net inductive voltage on the quench absorption coils is zero and no current transformation occurs. This situation changes if the top and bottom quench absorption coils are each grouped into separate circuits, as this would lead to a reduced effective inductance of the top and bottom superconducting coils and thus faster current oscillations. The implications of this are considered beyond the scope of this paper. It is also interesting to consider that in principle the presence of quench absorption coils allows for alternative means of applying the CLIQ concept, for instance by discharging a capacitor over half of the quench absorption coils and thus applying an external oscillating magnetic field to the superconducting coils. Another possibility involves discharging the superconducting coils over a dump resistor and periodically shorting this dump resistor with a thyristor. Then, current is repeatedly transformed back and forth between the primary and secondary circuits resulting in a coupling-loss-induced quench.

10. Conclusion

In this paper, the applicability of a concept called 'Quench Absorption Coils' for the quench protection of high-field dipoles is evaluated. This concept relies a placing copper-based coils in close proximity to superconducting coils, so that a significant fraction of the stored energy is dissipated in these coils during a quench. A finite-element model is used to evaluate the impact of this concept and a second numerical calculation is performed for consistency checks. Both calculations give consistent results, showing that the addition of coils constituting 36 % of the total winding volume absorb 45 % of the stored energy during a quench, thus reducing the peak hot spot temperature by over 100 K. In addition the presence of quench absorption coils results in a factor two reduction in the peak resistive voltage over the superconducting coils, thus reducing the required insulation performance. Due to its benefits this concept may prove useful for reducing the construction cost and enhancing the reliability of high-field accelerator magnets in which quench protection is a design driver.

[1] Enhanced European Coordination for Accelerator Research and Development Project, *http://eucard2.web.cern.ch/content/eucard*.

[2] F. Zimmermann, "LHEC and HE-LHC: Accelerator Layout and Challenges", Proc. of Chamonix 2012 workshop on LHC Performance, ISBN 978-92-9083-378-9, Chamonix (2012).

[3] FCC-hh baseline layout and parameter, *https://fcc.web.cern.ch/Pages/news/FCC-hh-baseline-layout-and-parameter.aspx*.

[4] P. H. Eberhard, M. Alston-Garnjost, M. A. Green, P. Lecomte, R. G. Smits, J. D. Taylor, and V. Vuillemin, "Quenches in Large Superconducting Magnets", LBNL report number 6718, (1977).

[5] M. A. Green, P. B. Eberhard, J. D. Taylor, W. A. Burns, B. Garfinkel, G. H. Gibson, P. B. Miller,

R. R. Ross, R. G. Smits, and H. W. Van Slyke, "A Magnet System for the Time Project Chamber at PEP", IEEE Trans. on Magnetics. 15, pp 128-130 (1979).

[6] M. N. Wilson, "Superconducting Magnets", Clarendon press, Oxford (1983).

[7] G. A. Kirby, J. van Nugteren, A. Ballarino, L. Bottura, N. Chouika, S. Clement, V. Datskov, L. Fajardo, J. Fleiter, R. Gauthier, L. Gentini, L. Lambert, M Lopes, J. C. Perez, G. de Rijk, A. Rijllart, L. Rossi, H. ten Kate, "Accelerator Quality HTS Dipole Magnet Demonstrator Designs for the EuCARD-2, 5 Tesla 40 mm Clear Aperture Magnet", IEEE Trans. on Appl. Supercond. 25, p. 4000805 (2015)

[8] M. Mentink, A. Dudarev, T. Mulder, J. van Nugteren, and H. ten Kate, "Quench Protection of Very Large, 50-GJ-Class and High-Temperature-Superconductor-Based Detector Magnets", IEEE Trans. on Appl. Supercond. 26, p. 4500608 (2016).

[9] L. Coull, D. Hagedorn, V. Remondino, and F. Rodriguez-Mateos, "LHC Magnet Protection System", IEEE Trans. on Magn. 30, pp. 1742-1745 (1994).

[10] G. Sabbi, S. E. Bartlett, S. Caspi, D. R. Dietderich, P. Ferracin, S. A. Gourlay, A. R. Hafalia, C. R. Hannaford, A. F. Lietzke, S. Mattafirri, A. D. McInturff, and R. Scanlan, "Design of HD2: A 15 Tesla Nb_3Sn Dipole with a 35 mm Bore", IEEE Trans. on Appl. Supercond. 15, p. 1128 (2005).

[11] P. Ferracin, S. Caspi, D. W. Cheng, D. R. Dietderich, A. R. Hafalia, C. R. Hannaford, H. Higley, A. F. Lietzke, J. Lizarazo, A. D. McInturff, and G. Sabbi, "Development of the 15 T Nb_3Sn dipole HD2', IEEE Trans. on Appl. Supercond. 18, p. 277 (2008).

[12] COMSOL Multiphysics, *https://www.comsol.com/comsol-multiphysics*.

[13] S. Sgobba, "Physics and Measurements of Magnetic Materials", Presented at CERN Accel. School CAS, arXiv:1103.1069, Bruges (2009).

[14] G. Manfreda, "Review of ROXIE's Material Properties Database for Quench Simulation", CERN internal note 2011-24, p. 1178007 (2011).

[15] G. S. Knapp, S. D. Bader, Z. Fisk, "Phonon Properties of A15 Superconductors Obtained from Heat-Capacity Measurements", Phys. Rev. B. 13, p. 37833789 (1976).

[16] L. Dresner, "Stability of Superconductors. Selected Topics in Superconductivity", Prenum Press, New York (1995).

[17] N. J. Simon, E. S. Drexler, and R. P. Reed, "Properties of Copper and Copper Alloys at Cryogenic Temperatures", NIST Monograph 177 (1992).

[18] E. D. Marquardt, J. P. Le, R. Radebaugh, "Cryogenic Material Properties Database", Cryocoolers 11, pp. 681-687 (2002).

[19] E. Ravaioli, H. Bajas, V. I. Datskov, V. Desbiolles, F. Feuvrier, G. Kirby, M. Maciejewski, G. Sabbi, H. ten Kate, and A. P. Verweij, "Protecting a Full-scale Nb_3Sn Magnet with CLIQ, the new Coupling-Loss-Induced Quench System", IEEE Trans. on Appl. Supercond. 25, p. 4001305 (2015).

[20] H. Bajas, M. Bajko, B. Bordini, L. Bottura, S. Izquierdo. Bermudez, J. Feuvrier, A. Chiuchiolo, J. C. Perez, and G. Willering, "Quench Analysis of High-Current-Density Nb_3Sn Conductors in Racetrack Coil Configuration", IEEE Trans. on Appl. Supercond. 25, p. 4004005 (2015).

[21] D. Leroy, J. Krzywinski, V. Remondino, L. Walckiers, and R. Wolf, "Quench Observation in LHC Superconducting One Meter Long Dipole Models by Field Perturbation Measurements", IEEE Trans. on Appl. Supercond. 3, pp. 781-784 (1993).

[22] S. Jongeleen, D. Leroy, A. Siemko, and R. Wolf, "Quench Localization and Current Redistribution after Quench in Superconducting Dipole Magnets Wound with Rutherford-type Cables", LHC Project Report 59 (1996).

[23] J. van Nugteren, G. Kirby, G. de Rijk, and L. Rossi, "Aligned Coil Block: A New Design for HTS Magnets", CERN report CERN-ACC-SLIDES-2014-0042, p. 1 (2014).

[24] L. Bottura, P. Pugnat, A. Siemko, J. Vlogaert, and C. Wyss, "Performance of the LHC Final Design Full Scale Superconducting Dipole Prototypes", IEEE Trans. on Appl. Supercond. 11, p. 1554 (2001).

[25] E. Todesco, "Quench limits in the Next Generation of Magnets", CERN Yellow Report CERN-

2013-006 (2013).

[26] F. Total, L. Garcia-Tabares, T. Martinez, J. Munilla, J. Ruuskanen, T. Salmi, and A. Stenvall, "EuroCirCol 16 T Common-Coil Dipole Option for the FCC", IEEE Trans. on Appl. Supercond. 27, p. 4001105 (2017).

[27] V. Marinozzi, G. Bellomo, B. Caiffi, P. Fabbricatore, S. Farinon, T. Salmi, M. Sorbi, A. Stenvall, and G. Volpini, "Quench Protection Study of the EuroCirCol 16 T cosθ Dipole for the Future Circular Collider (FCC)", IEEE Trans. on Appl. Supercond. 27, p. 2656156 (2017).

[28] C. Lorin, M. Durante, and M. Segreti, "EuroCirCol 16 T Block-Coils Dipole Option for the Future Circular Collider", IEEE Trans. on Appl. Supercond. 27, p. 4001405 (2017).

[29] G. Moritz, "Eddy Currents in Accelerator Magnets", CERN document CERN-2010-004, arXiv:1103.1800, pp. 103-140 (2010).

[30] J. van Nugteren, J. Murtomaki, G. Kirby, P. Hagen, G. de Rijk, H. ten Kate, and L. Rossi, "E3presso, a Quench Protection System for High Field Superconducting Magnets", CERN internal note: 2016-23 (2016).